

# Selective Recovery of Precious Metals through Photocatalysis

**Yao Chen**

Shanghai Normal University

**Mengjiao Xu**

Shanghai Normal University

**Jieya Wen**

Shanghai Normal University

**Yu Wan**

Shanghai Normal University

**Qingfei Zhao**

Shanghai Normal University

**Xia Cao**

Beijing Institute of Nanoenergy and Nanosystems

**Yong Ding**

Georgia Institute of Technology

**Zhong Wang**

Georgia Institute of Technology

**Hexing Li** (✉ [hexing-li@shnu.edu.cn](mailto:hexing-li@shnu.edu.cn))

Shanghai Normal University

**Zhenfeng Bian**

Shanghai Normal University <https://orcid.org/0000-0001-7552-8027>

---

## Article

**Keywords:** precious metals, photocatalysis, selective recovery

**Posted Date:** August 31st, 2020

**DOI:** <https://doi.org/10.21203/rs.3.rs-66024/v1>

**License:** © ⓘ This work is licensed under a Creative Commons Attribution 4.0 International License.

[Read Full License](#)

---

**Version of Record:** A version of this preprint was published at Nature Sustainability on March 25th, 2021.  
See the published version at <https://doi.org/10.1038/s41893-021-00697-4>.

# 1            **Selective Recovery of Precious Metals through Photocatalysis**

2    Yao Chen<sup>1</sup>, Mengjiao Xu<sup>1</sup>, Jieya Wen<sup>1</sup>, Yu Wan<sup>1</sup>, Qingfei Zhao<sup>1</sup>, Xia Cao<sup>3</sup>, Yong Ding<sup>4</sup>,  
3    Zhong Lin Wang<sup>3,4\*</sup>, Hexing Li<sup>1,2\*</sup> & Zhenfeng Bian<sup>1\*</sup>

4    <sup>1</sup> MOE Key Laboratory of Resource Chemistry and Shanghai Key Laboratory of Rare  
5    Earth Functional Materials, Shanghai Normal University, Shanghai 200234, China.

6    <sup>2</sup> Shanghai University of Electric Power, Shanghai 200090, China.

7    <sup>3</sup> Beijing Institute of Nanoenergy and Nanosystems, Chinese Academy of Sciences,  
8    Beijing 100083, China.

9    <sup>4</sup> School of Materials Science and Engineering, Georgia Institute of Technology,  
10    Atlanta, Georgia 30332-0245, United States.

11    **Precious metals such as gold and platinum are valued materials for a variety of**  
12    **important applications, but their scarcity poses a risk of supply interruption.**  
13    **However, the dissolution and recovery of precious metals using the current**  
14    **methods are limited by associated serious environmental pollution and high**  
15    **energy consumption. Here, we show a photocatalytic process that allows one to**  
16    **selective retrieve 7 kinds of precious metal elements (Ag, Au, Pd, Pt, Ru, Rh and**  
17    **Ir) (with dissolution efficiency of 99%) from waste circuit boards, ternary**  
18    **automotive catalysts and even ores. Precious metals is recovered with high purity**  
19    **(≥98%) through a simple reductive method. The whole process only needs light**  
20    **and catalyst without strong acid, strong base and highly toxic cyanide. It has an**  
21    **environmentally friendly, scalable and efficient way, in which the catalyst has been**  
22    **recycled more than 100 times under normal temperature and pressure without**  
23    **performance degradation. It has successfully realized the scale of dissolution from**  
24    **grams to kilograms, and it is expected to realize large-scale recovery of precious**  
25    **metals in industrial application. This general approach provides an unprecedent**  
26    **technology for recycling resources on earth.**

## 27 **Introduction**

28 Precious metals (PMs) possess not only good physical properties (ductility,  
29 electrical conductivity), but also high chemical stability and strong corrosion  
30 resistance<sup>1</sup>. In recent years, precious metals have been increasingly used in the fields of  
31 electronic devices and modern industrial catalysis<sup>2,3</sup> etc. It is reported that the global  
32 demand for gold, silver and palladium in the electronics industry was about 250 tons,  
33 12,800 tons and 40 tons, respectively<sup>4-6</sup>. In addition, due to the continuous development  
34 of the automobile industry, the consumption of platinum group metals is increasing<sup>5</sup>.  
35 The global electronic waste (e-waste) production shows that the gold content in 40  
36 mobile phones is equivalent to one ton of ore<sup>7</sup>. In 2019, a total of 53.6 million tons of  
37 precious metal-containing e-waste were generated globally, including discarded  
38 computers, mobile phones and households electronic equipment<sup>8,9</sup>. It is a very  
39 meaningful to recycle precious metals from e-waste and waste catalyst.

40 It remains a grand challenge to mine and retrieve precious metals from ores,  
41 catalysts and electronic wastes for reusage<sup>10-13</sup>. The recovery process of precious metal  
42 is divided into two steps: firstly, dissolve  $PM^0$  into  $PM^{x+}$  from electronic wastes; then  
43 reduce  $PM^{x+}$  to  $PM^0$  from the leachate. In the process of dissolving  $PM^0$  to  $PM^{x+}$ ,  
44 dissolution methods in the industry involving the use of corrosive and toxic aqua regia  
45 and cyanidation endanger the environment and characterized of high chemical  
46 consumption<sup>14-18</sup>. In view of the toxicity of aqua regia and cyanide, scientists have  
47 developed non-toxic leaching agents such as thiourea, thiosulfate and iodine to treat the  
48 dissolution of gold, but they are ineffective for the dissolution of platinum group  
49 precious metals and the operation steps are complicated (Extended Data Table 1)<sup>18-23</sup>.  
50 Moreover, Yang et al. used n-bromosuccinimide (NBS) and pyridine (Py) directly  
51 leached  $Au^0$  waste to form  $Au^{III}$  from gold ore and electronic<sup>24</sup>. Hong et al. used sulfuryl  
52 chloride ( $SOCl_2$ ) and some organic solvents/reagents (pyridine, N, N-  
53 dimethylformamide and imidazole) to form "organic aqua regia" to dissolve gold and  
54 palladium<sup>25</sup>. The limitation of the above method is that it can only dissolve one or two  
55 precious metals and the reagent composition is complicated, which not only increases

56 the difficulty of actual operation, but also increases the cost of recovery. In the process  
57 of reducing  $PM^{x+}$  to  $PM^0$ , scientists usually design materials that can withstand acid to  
58 extract precious metal ions. Hong et al. reported a porous porphyrin polymer which can  
59 quantitatively capture precious metals ion from the acidic exudate of e-waste<sup>26</sup>. The  
60 existing methods in the literature can achieve selective reduction of a precious metal.  
61 Smith et al. used 1,3:2,4-dibenzylidenesorbitol as a raw material to prepare a hydrogel  
62 material capable of extracting gold/silver ions<sup>27</sup>. Queen et al. prepared Fe-BTC/PpPDA  
63 composite material, which was proven to quickly extract trace amounts of gold ion from  
64 water mixtures<sup>28</sup>. In fact, the dissolution process of precious metals is more difficult to  
65 achieve than reduction because precious metals are chemically inert, which require  
66 strong oxidizing reagents.

67 It has been reported that the photocatalysis can generate highly reactive free  
68 radicals in the reaction system under mild conditions. Moreover, the photocatalytic  
69 technology has the advantages of simple operation, low energy consumption, no  
70 secondary pollution and high efficiency. Photocatalytic oxidation has become a  
71 technology of choice to tackle environmental pollution and energy crisis due to its direct  
72 utilization of solar light-driven reaction and good catalyst stability. The oxidizing  
73 ability of photo-generated holes ( $TiO_2$  ( $2.91 V_{NHE}$ )) is sufficient to oxidize  $PM^0$  into  
74  $PM^{x+}$  ( $Rh$  ( $0.75 V_{RHE}$ ) <  $Ir$  ( $0.9 V_{RHE}$ ) <  $Pt$  ( $1.1 V_{RHE}$ ) <  $Au$  ( $1.3 V_{RHE}$ ))<sup>29,30</sup>. But so far,  
75 there is no report on the oxidation and dissolution of precious metals by photocatalytic  
76 method.

77 Here, we have realized the use of photocatalysis to dissolve precious metals,  
78 without strong acids, strong bases and toxic solvents. It has good leaching effect for 7  
79 kinds of precious metals ( $Ag$ ,  $Au$ ,  $Pd$ ,  $Pt$ ,  $Ru$ ,  $Rh$  and  $Ir$ ). Interestingly, selective  
80 dissolution of precious metals can also be achieved, providing an easy way of  
81 separating these metals. More importantly, this photocatalytic technology for  
82 dissolving precious metals can not only realize the recovery of noble metal nano-  
83 catalysts in the laboratory, but also effectively leached precious metals from e-waste,  
84 ore and automobile three-way catalyst on a large scale. To our best knowledge, this is

85 the first time that an environmental friendly photocatalysis has been applied to the  
86 dissolution and recovery of precious metals.

87

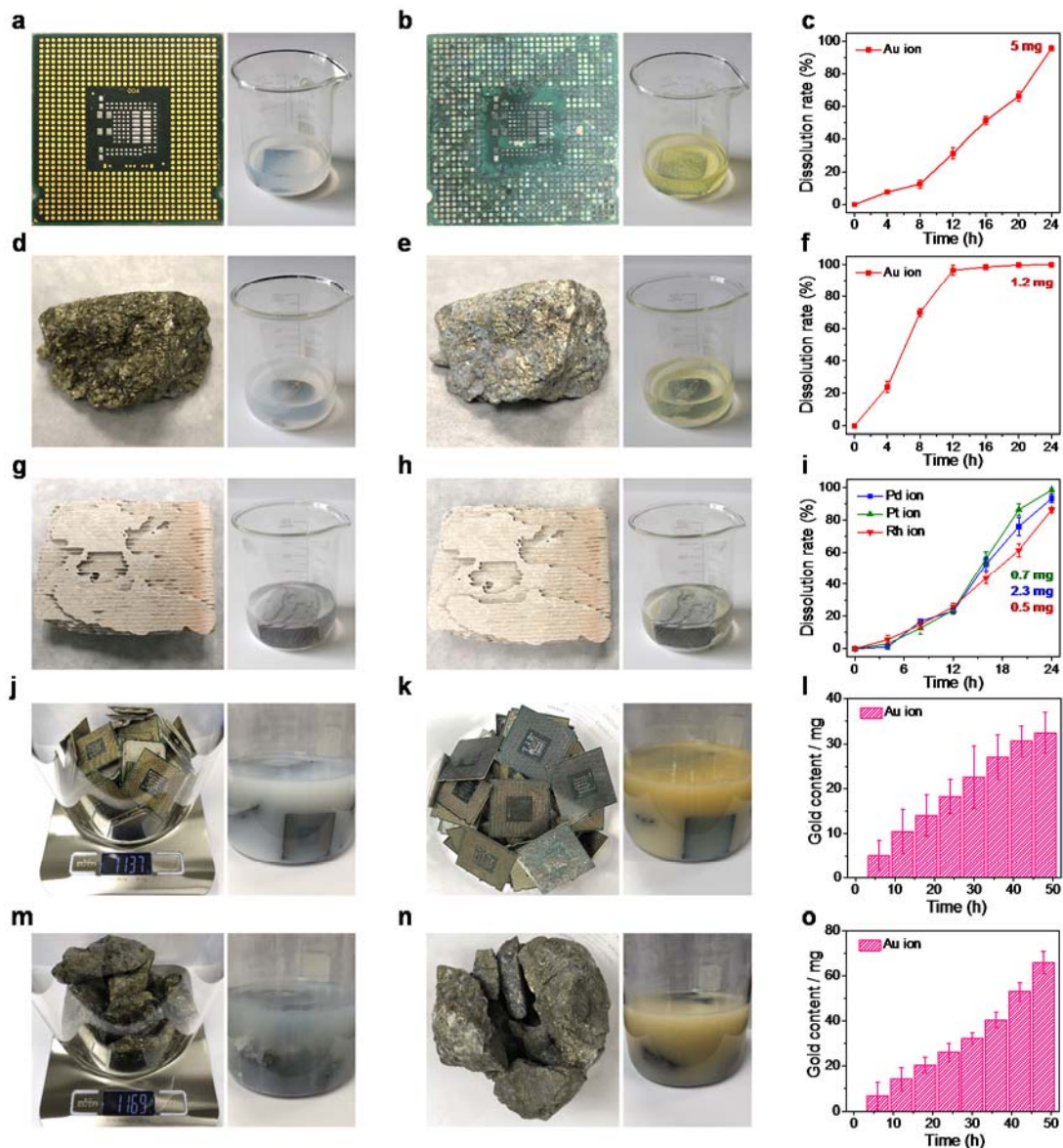
## 88 **Results**

### 89 **Photocatalytic Dissolution of Precious Metals**

90 Here, photocatalysis was used to recycle precious metals from waste electrical and  
91 electronic equipment (WEEE), ore waste and three-way catalytic (TWC). As shown in  
92 **Fig. 1**, gold (Au) from central processing unit (CPU) board (**Fig. 1a-1c**) and gold ore  
93 (**Fig. 1d-1f**) was successfully dissolved by light irradiation, as well as palladium (Pd),  
94 platinum (Pt) and rhodium (Rh) contained in TWC (**Fig. 1g-1i**). The required reaction  
95 conditions are mild and the raw materials can be simply added and mixed (**Extended**  
96 **Data Fig. 1**). By crushing the bulk samples, the reaction contact surface can be  
97 increased and more metals will be dissolved out (**Extended Data Fig. 2**). As shown in  
98 **Extended Data Fig. 3**, there are several metals such as copper (Cu), nickel (Ni) and  
99 gold (Au) in the CPU board. In the process of photocatalytic dissolution, these non-  
100 noble metals can also be dissolved (**Extended Data Fig. 4**). Compared with the aqua  
101 regia method, the photocatalytic process has a mild reaction. The dissolution process of  
102 aqua regia reacts violently and produces a large amount of toxic and harmful substances,  
103 such as chlorine. The fracture of CPU block was seriously cracked (**Extended Data**  
104 **Fig. 5**).

### 105 **Scalability Dissolution of Precious Metals**

106 The whole dissolution process is very simple, and the scale of the experiment can  
107 be easily increased to the kilogram level. Take CPU and gold ore as examples (**Fig. 1j-**  
108 **1o**), we used 1.137 kg of CPU board and 1.169 kg of ore respectively. With the increase  
109 of reaction time, the content of gold in the solution increased gradually. The color of  
110 the solution showed the yellow characteristic of gold ions. These showed that the  
111 method is feasible in scale-up.



112

113 **Figure 1 | Photocatalytic dissolution of precious metals from CPU board, gold ore**  
 114 **and TWC.** Photographs of retrieving gold from CPU board (a) before and (b) after  
 115 reaction. Photographs of retrieving gold from gold ore (28.8 g) (d) before and (e) after  
 116 reaction. Photographs of retrieving precious metals from TWC (17.9 g) (g) before and  
 117 (h) after reaction. Photographs of retrieving gold from CPU board (1.137 kg) (j) before  
 118 and (k) after reaction. Photographs of retrieving gold from ore (1.169 kg) (m) before  
 119 and (n) after reaction. The amount of precious metals obtained by photocatalyzing  
 120 unbroken CPU board (c) (l), gold ore (f) (o) and TWC (i).

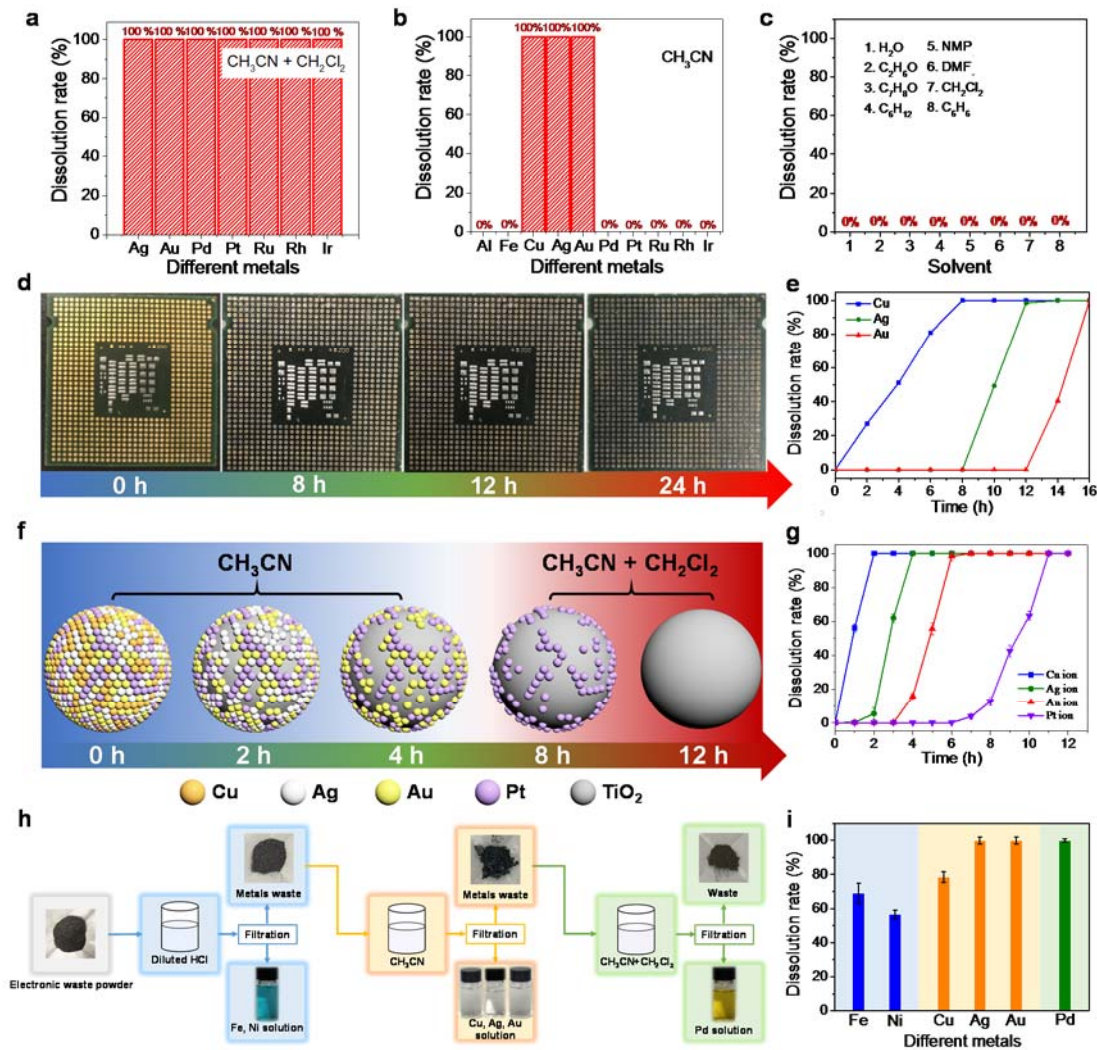
121

## 122 **Selective Dissolution of Precious Metals**

123 We investigated the dissolution rate of different solvents for different metals under  
124 photocatalytic conditions. In the mixed system of acetonitrile (MeCN) and  
125 dichloromethane (DCM), 7 kinds of precious metals (Au, Ag, Pd, Pt, Ru, Rh and Ir)  
126 can be effectively dissolved under light irradiation (**Fig. 2a and Extended Data Fig.**  
127 **6**). While only Au, Ag and Cu can be dissolved in MeCN under the same conditions.  
128 (**Fig. 2b**). Through screening 9 kinds of common solvents, it is found that only MeCN  
129 can be used as solvent to realize this dissolution process (**Fig. 2c**). The selective  
130 dissolution of precious metals was achieved by adjusting the reaction solvent and  
131 reaction time. Taking the CPU board as the research object, the results showed that Cu,  
132 Ag and Au on CPU board dissolved step by step with the increase of irradiation time  
133 (**Fig. 2d-2e**).

134 To evaluate the selectivity of photocatalytic dissolution, TiO<sub>2</sub> samples loaded with  
135 commonly used metals Cu, Ag, Au and Pt were selected as the research object. As  
136 shown in **Figure 2f and 2g**, we sequentially dissolved Cu, Ag and Au in MeCN by  
137 controlling the reaction time, then Pt is further dissolved by adding DCM. Finally, we  
138 choose the e-waste powder, which contains Fe, Ni, Cu, Ag, Au and Pd. By adjusting  
139 the solvent and reaction time, we can selectively recover the precious metals Ag, Au  
140 and Pd (**Fig. 2h-2i**).





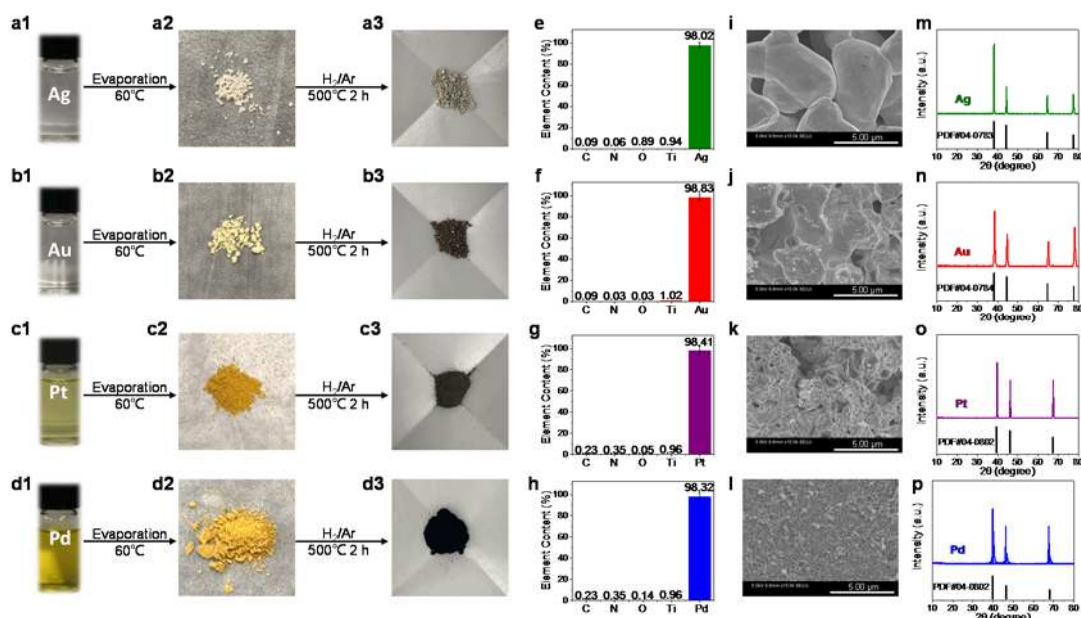
141

142 **Figure 2 | Photocatalytic selective dissolution of metals.** (a) Dissolution rate of Ag,  
 143 Au, Pd, Pt, Ru, Rh and Ir in the mixed system of MeCN and DCM under photocatalytic  
 144 conditions. (b) Dissolution rate of Al, Fe, Cu, Ag, Au, Pd, Pt, Ru, Rh and Ir in MeCN  
 145 under photocatalytic conditions. (c) Dissolution rate of Au in different solution. (d)  
 146 Photographs of selective retrieving metal from CPU board. (f) Schematic diagram of  
 147 selective dissolution process of metals catalyst (1% Cu/TiO<sub>2</sub>, 1% Ag/TiO<sub>2</sub>, 1% Au/TiO<sub>2</sub>  
 148 and 1% Pt/TiO<sub>2</sub>). (h) Flow-sheet of stepwise extraction of Fe, Ni, Cu, Ag, Au and Pd  
 149 from e-waste powder. The amount of metals obtained by selective photocatalyzing (e)  
 150 CPU board, (g) metals catalyst and (i) e-waste powder.

151

152 **Reduction Recovery of Precious Metal Ion**

153 There are many ways to reduce  $PM^{x+}$  to  $PM^0$ , such as hydrogen reduction, thermal  
 154 reduction, and reducing agents. Here, we choose the simplest hydrogen reduction  
 155 method, which can directly obtain the precious metals. The reduction process is divided  
 156 into two steps: the first is to recycle the solvent, and the second is to reduce the  
 157 precipitated solid to the precious metal. (**Fig. 3a-3d**). The analysis shows that the purity  
 158 of the recovered precious metals is more than 98% (**Fig. 3e-3h**). Scanning electron  
 159 microscopy (SEM) shows that the precious metals are nanoparticles (**Fig. 3i-3l**). X-ray  
 160 diffraction (XRD) further proved that these samples were metal Ag, Au, Pt and Pd,  
 161 respectively (**Fig. 3m-3p**).



162  
 163 **Figure 3 | Precious metal ion reduction process.** The solvent of the dissolved product  
 164 is removed and then calcined in a reducing atmosphere to obtain metal (a) Ag, (b) Au,  
 165 (c) Pt and (d) Pd. The proportion of metal elements in the (e) Ag, (f) Au, (g) Pt and (h)  
 166 Pd after roasting. SEM image of the reduced product (i) Ag, (j) Au, (k) Pt and (l) Pd.  
 167 XRD pattern of the reduced product (m) Ag, (n) Au, (o) Pt and (p) Pd.

168

## 169 Discussion

170 In order to understand the mechanism of photocatalytic dissolution of precious  
 171 metals, some controlled experiments have been conducted. A commercial 5% Pt/C

172 sample is used first for photocatalyzing precious metals dissolution. Photocatalysts  
173 (TiO<sub>2</sub>) and precious metal catalysts (5% Pt/C) are directly mixed in solvents and stirred  
174 (**Extended Data Fig. 7**). As shown in **Fig. 4a**, Pt nanoparticles are evenly distributed  
175 on carbon surface. Pt nanoparticles disappeared from the surface after UV light  
176 illumination (**Fig. 4b**). This can be further analyzed based on the analysis of the  
177 elements in the solution, which shows that the content of Pt gradually increases in the  
178 solution and Pt is completely dissolved after 4 hours (**Fig. 4g**, red line). The change of  
179 Pt content on the surface was further analyzed by XPS spectra<sup>23</sup>. As the reaction  
180 proceeded, the binding energies of Pt<sup>0</sup> 4f dropped substantially (**Fig. 4c**)<sup>31</sup>. To further  
181 analyze the structure of the product, we removed the solvent from the reaction solution  
182 (after reaction 4 h) and extracted the luminous the yellow powder sample (**Extended**  
183 **Data Fig. 8a**). The infrared spectrum of the powder extracted from the solution after  
184 the reaction confirmed the formation of new materials species (**Fig. 4d**). By comparing  
185 the infrared spectra of the solution after the reaction, a new infrared absorption peak  
186 appeared in the powder sample, located in the region of 3344–2913 cm<sup>-1</sup>, which is a  
187 typical N–H stretching vibration peak<sup>32</sup>. Moreover, the original C–N peak disappeared,  
188 which indicates that MeCN can react to form a substance containing N–H bond during  
189 the dissolution process<sup>33</sup>. X-ray diffraction (XRD) analysis of powder samples showed  
190 that the diffraction of ((NH<sub>4</sub>)<sub>x</sub>PtCl<sub>y</sub>) sample has the hexachloroplatinate structure  
191 ((NH<sub>4</sub>)<sub>2</sub>PtCl<sub>6</sub>) (PDF#07-0218)) (**Fig. 4e**). Compared with the commercial (NH<sub>4</sub>)<sub>2</sub>PtCl<sub>6</sub>,  
192 the powder samples have similar colors and XRD peak shapes (**Extended Data Fig.**  
193 **8b–8c**). The N–H peak in powder infrared should be the amino vibration peak in this  
194 sample. Energy disperse spectroscopy (EDS) mapping analysis demonstrated that there  
195 were only three elements (N, Cl, Pt) in powder samples (**Extended Data Fig. 9**), which  
196 is consistent with the results of XRD. X-ray photoelectronic spectroscopy (XPS)  
197 analysis further showed that the valence states of platinum in the sample were mainly  
198 tetravalent and divalent (Pt<sup>4+</sup> (73.4 eV and 75.3 eV) and Pt<sup>2+</sup> (76.7 eV and 78.6 eV))  
199 (**Fig. 4f**)<sup>34</sup>. The N and Cl elements also exhibit corresponding peaks of N–H and Pt–Cl  
200 (**Extended Data Fig. 10**). Through electron paramagnetic resonance (EPR) test of the  
201 solution, the valence states of platinum in the sample might also have a small amount

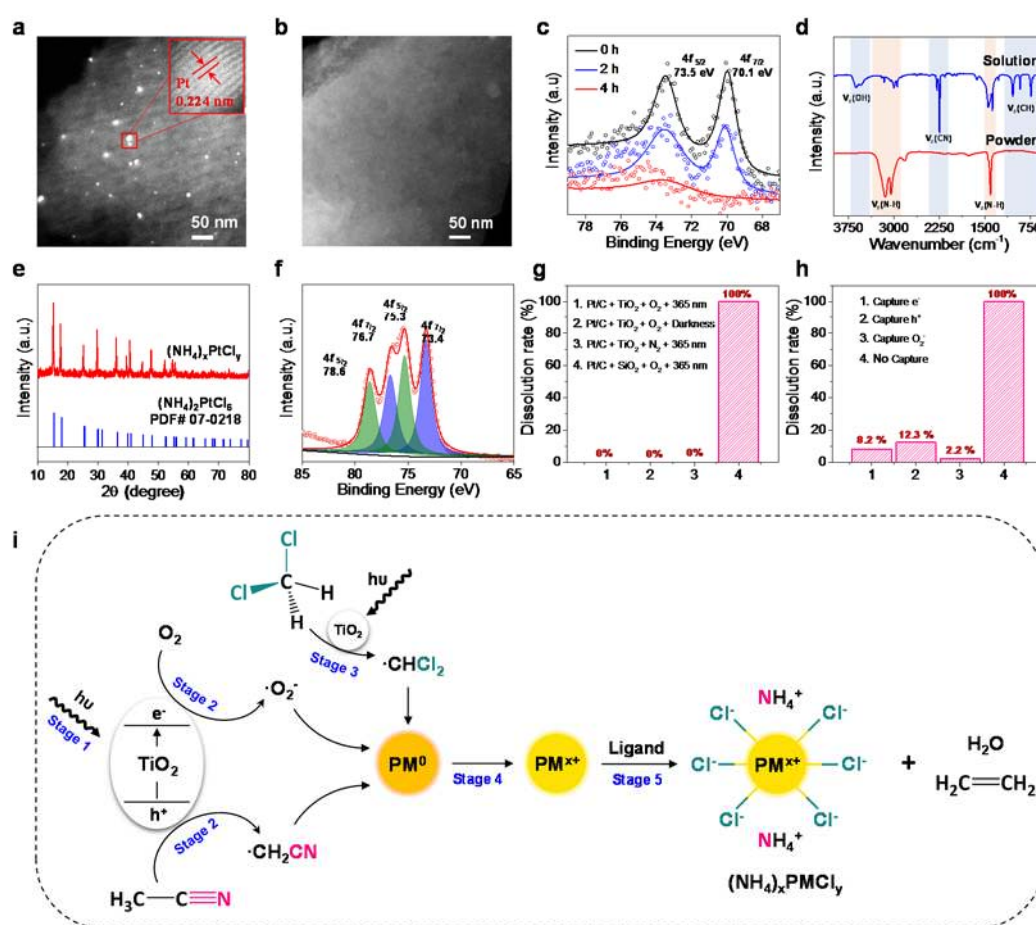
202 of Pt<sup>+</sup> or Pt<sup>3+</sup> (**Extended Data Fig. 11**)<sup>35</sup>. From the valence state of Pt, it shows that Pt  
203 has been oxidized from Pt<sup>0</sup> to Pt<sup>4+</sup>.

204 Platinum nanoparticles (Pt NPs) on different supports (SiO<sub>2</sub>, Al<sub>2</sub>O<sub>3</sub> and molecular  
205 sieve) can be dissolved by photocatalytic technology (**Extended Data Fig. 12**). The  
206 main function of the TiO<sub>2</sub> is to produce active species under light irradiation. Other  
207 photocatalysts, such as ZnO (under UV light irradiation) or CdS (under visible light  
208 irradiation), can also realize the dissolution of Pt NPs (**Extended Data Fig. 13**).  
209 Through the study of the content and change of various solvents, it indicates the  
210 importance of cyano group and chloric substituent (**Extended Data Fig. 14**). The  
211 aqueous solution of ammonium chloride cannot dissolve Pt NPs through photocatalytic  
212 technology, and the inorganic chloride is also ineffective for the dissolution of Pt NPs  
213 (**Extended Data Fig. 15**). The control experiments indicate that the presence of oxygen,  
214 UV light, and photocatalyst is essential for Pt NPs dissolution (**Fig. 4g**). According to  
215 the dissolution efficiency of capturing electrons (the superoxide radicals ( $\bullet\text{O}_2^-$ ) formed  
216 by the combination with oxygen) and holes (**Fig. 4h**), the photogenerated electrons and  
217 holes are the main active charge carriers.

218 In addition, the  $\bullet\text{O}_2^-$  and methyl radicals ( $\bullet\text{CH}_2\text{R}$ ) generated during the reaction  
219 were further verified by ESR test (**Extended Data Fig. 16a**). Under the condition of no  
220 photocatalyst, free radical is not detected (**Extended Data Fig. 16b**). Further, the  
221 content of hydrogen peroxide (H<sub>2</sub>O<sub>2</sub>) in the system was not detected by the iodometric  
222 method, proving that the superoxide radical has not been converted to H<sub>2</sub>O<sub>2</sub> (**Extended**  
223 **Data Fig. 17**). Through a comprehensive analysis of the dissolution system, acetylene  
224 was found in the gas phase (**Extended Data Fig. 18**). The experiments of discolored  
225 silica gel were used to prove that there was water in the solution after reaction, and the  
226 water content in the dissolution reaction is quantitatively detected by Karl Fischer  
227 analysis. (**Extended Data Fig. 19**).

228 Based on the above results, the reaction mechanism of the photocatalyzing  
229 dissolution process is proposed in **Fig. 4i**. Photogenerated electrons and holes on TiO<sub>2</sub>  
230 are first excited by UV light (stage 1). Photogenerated electrons react with oxygen

231 molecules to form  $\bullet\text{O}_2^-$  (stage 2)<sup>36</sup>. Holes react with MeCN in mixed solvents to  
 232 deprotonate into  $\bullet\text{CHCN}$  radical (stage 2). DCM decomposes into  $\bullet\text{CH}_2\text{Cl}$  with strong  
 233 oxidizing ability under the excitation of light (stage 3). These active species oxidize  
 234  $\text{PM}^0$  to form  $\text{PM}^{x+}$  (stage 4). At the same time, the solvent is decomposed into acetylene,  
 235 amino group and water. Finally, the ions coordinate with each other to form  
 236  $(\text{NH}_4)_x\text{PMCl}_y$  (stage 5). The dissolved products of Cu and Au also have similar  
 237 compound structures, which further verifies the reliability of the mechanism. The XPS  
 238 spectra of Cu and Au show that the metal is ionized after dissolution (**Extended Data**  
 239 **Fig. 20a and 20b**). The XRD patterns of Cu compound correspond ammonium  
 240 chlorocuprate  $(\text{NH}_4)_2\text{CuCl}_4 \cdot 2\text{H}_2\text{O}$  (**Extended Data Fig. 20c**). It can be shown that the  
 241 Au product should be  $(\text{NH}_4)_x\text{AuCl}_y$  by data fitting (**Extended Data Fig. 20d**). The  
 242 oxidation potential and coordination environment were changed by the regulation of  
 243 solvent. Therefore, the selective dissolution of Cu, Ag and Au in MeCN can be realized  
 244 by adjusting the solvent.



246 **Figure 4 | Exploration of mechanism.** High-angle annular dark-field (HAADF)  
247 scanning transmission electron microscopy (STEM) images of 5% Pt/C (a) before and  
248 (b) after reaction. (c) The Pt element distribution in Pt/C sample determined by XPS  
249 spectra with reaction time. (d) FTIR spectra of solution and powder sample after  
250 reaction. (e) XRD patterns and (f) Pt 4f7 XPS spectra of Pt compound obtained from  
251 the solution. (g) Dissolution rate of Pt under different conditions. (h) Dissolution rate  
252 of Pt under the capture of different living species (DDQ capture electrons ( $e^-$ ), EDTA-  
253 2Na capture holes ( $h^+$ ), p-benzoquinone capture superoxide radical ( $\bullet O_2^-$ )). (i) Proposed  
254 mechanism for the retrieving precious metal by photocatalysis.

255 In this work, we are able to take the advantage of the photocatalytic oxidation  
256 technology to solve the complete and selective dissolution of precious metals under  
257 mild conditions. We realized the oxidation leaching of precious metal ions from e-waste,  
258 ore and TWC, and then recovered the precious metals. The method is simple, mild and  
259 environmentally friendly, and is suitable for all kinds of precious metals. It indicated  
260 that the whole reaction process is stable and can be recycled. The reaction solvent can  
261 be continuously circulated for more than 45 times (**Extended Data Fig. 21**). In addition,  
262 the photocatalyst can be recycled more than 100 times (**Extended Data Fig. 22a**). The  
263 morphology and structure of the photocatalyst did not change before and after the  
264 reaction (**Extended Data Fig. 22b and 22c**), and no free form of Ti ions was detected  
265 in the solution after dissolution (**Extended Data Fig. 22d**). Such a general method has  
266 a wide range of applications and can be applied not only to the recovery of precious  
267 metals from powder nanocatalysts, but also the recovery of precious metals from WEEE,  
268 mining of precious metals ores and TWC. It provides a breakthrough solution for the  
269 smelting, dissolution and recovery of precious metals, and broadens the application  
270 field of photocatalysis.

271

272 **Data availability**

273 The data supporting the findings of the study are available within the paper and its  
274 Supplementary Information.

275 **References**

- 276 1. Fan, Z. & Zhang, H. Crystal phase-controlled synthesis, properties and  
277 applications of noble metal nanomaterials. *Chem. Soc. Rev.* **45**, 63-82 (2016).
- 278 2. Zhao, M. *et al.* Metal-organic frameworks as selectivity regulators for  
279 hydrogenation reactions. *Nature* **539**, 76-80 (2016).
- 280 3. Sean T. Hunt *et al.* Self-assembly of noble metal monolayers on transition metal  
281 carbide nanoparticle catalysts. *Science* **352**, 947-978 (2019).
- 282 4. USGS, Commodity Statistics and Information, 2017.  
283 <https://minerals.usgs.gov/minerals/pubs/commodity/>.
- 284 5. Li, B. *et al.* Recovery of platinum group metals from spent catalysts: A review.  
285 *Int. J. Miner. Process.* **145**, 108-113 (2015).
- 286 6. NIMS (National Institute for Material Science, Japan), 2015. Available at:  
287 [www.nims.go.jp/jpn/news/press/pdf/press215\\_2.pdf](http://www.nims.go.jp/jpn/news/press/pdf/press215_2.pdf).
- 288 7. Cafer T. Yavuz *et al.* Gold Recovery from E-Waste by Porous  
289 Porphyrin-Phenazine Network Polymers. *Chem. Mater.* **32**, 5343-5349 (2020).
- 290 8. Liu, C. *et al.* Economic and environmental feasibility of hydrometallurgical  
291 process for recycling waste mobile phones. *Waste Manage.* **111**, 41-50 (2020).
- 292 9. Prudence Dato. Economic analysis of e-waste market. *Int Environ Agreements.*  
293 **17**, 815-837 (2017).
- 294 10. Doidge, E. D. *et al.* A simple primary amide for the selective recovery of gold  
295 from secondary resources. *Angew. Chem. Int. Ed.* **55**, 12436-12439 (2016).
- 296 11. Sun, D. T., Gasilova, N., Yang, S., Oveisi, E. & Queen, W. L. Rapid, selective  
297 extraction of trace amounts of gold from complex water mixtures with a metal-  
298 organic framework (MOF)/polymer composite. *J. Am. Chem. Soc.* **140**, 16697-  
299 16703 (2018).



- 300 12. Liu, Z. *et al.* Selective isolation of gold facilitated by second-sphere  
301 coordination with alpha-cyclodextrin. *Nat. Commun.* **4**, 1855 (2013).
- 302 13. Yue, C. *et al.* Environmentally benign, rapid, and selective extraction of gold  
303 from ores and waste electronic materials. *Angew. Chem. Int. Ed.* **56**, 9331-9335  
304 (2017).
- 305 14. Cherevko, S. *et al.* Dissolution of noble metals during oxygen evolution in  
306 acidic media. *ChemCatChem* **6**, 2219-2223 (2014).
- 307 15. McGivney, E. *et al.* Biogenic cyanide production promotes dissolution of gold  
308 nanoparticles in soil. *Environ. Sci. Technol.* **53**, 1287-1295 (2019).
- 309 16. Birich, A., Stopic, S. & Friedrich, B. Kinetic investigation and dissolution  
310 behavior of cyanide alternative gold leaching reagents. *Sci Rep* **9**, 7191 (2019).
- 311 17. Ahtiainen, R. & Lundström, M. Cyanide-free gold leaching in exceptionally  
312 mild chloride solutions. *J. Clean Prod.* **234**, 9-17 (2019).
- 313 18. James Hutton: father of modern geology, *Nature* **119**, 1726–1797 (1927).
- 314 19. Lee, H., Molstad, E. & Mishra, B. Recovery of gold and silver from secondary  
315 sources of electronic waste processing by thiourea leaching. *JOM* **70**, 1616-  
316 1621 (2018).
- 317 20. Burdinski, D. & Bles, M. H. Thiosulfate- and thiosulfonate-based etchants for  
318 the patterning of gold using microcontact printing. *Chem. Mater.* **19**, 3933-3944  
319 (2007).
- 320 21. Cho, E. C., Xie, J., Wurm, P. A. & Xia, Y. Understanding the role of surface  
321 charges in cellular adsorption versus internalization by selectively removing  
322 gold nanoparticles on the cell surface with a I<sub>2</sub>/KI etchant. *Nano Lett.* **9**, 1080-  
323 1084 (2009).
- 324 22. Parga, J. R., Valenzuela, J. L. & T., F. C. Pressure cyanide leaching for precious  
325 metals recovery. *JOM* **59**, 43–47 (2007).
- 326 23. Lopes, P. P. *et al.* Dynamics of electrochemical Pt dissolution at atomic and  
327 molecular levels. *J. Electroanal. Chem.* **819**, 123-129 (2018).



- 328 24. Peng, Y. *et al.* Environmentally Benign, Rapid, and Selective Extraction of Gold  
329 from Ores and Waste Electronic Materials. *Angew. Chem. Int. Ed.* **56**, 9331 –  
330 9335 (2017).
- 331 25. Hong, J. *et al.* “Organic Aqua Regia”—Powerful Liquids for Dissolving Noble  
332 Metals. *Angew. Chem. Int. Ed.* **49**, 7929 –7932 (2010).
- 333 26. Hong, Y. *et al.* Precious Metal Recovery from Electronic Waste by a Porous  
334 Porphyrin Polymer. *PNAS* **117** (28), 16174-16180 (2020).
- 335 27. David K. Smith. *et al.* Selective Extraction and In Situ Reduction of Precious  
336 Metal Salts from Model Waste To Generate Hybrid Gels with Embedded  
337 Electrocatalytic Nanoparticles. *Angew. Chem. Int. Ed.* **55**, 183 –187 (2016).
- 338 28. Wendy L. Queen. *et al.* Rapid, Selective Extraction of Trace Amounts of Gold  
339 from Complex Water Mixtures with a Metal–Organic Framework  
340 (MOF)/Polymer Composite. *J. Am. Chem. Soc.* **140**, 48, 16697–16703 (2018).
- 341 29. Wang, X. *et al.* Semiconductor Heterojunction Photocatalysts: Design,  
342 Construction, and Photocatalytic Performances. *Chem. Soc. Rev.* **43**, 5234  
343 (2014).
- 344 30. Serhiy, C. *et al.* Dissolution of Noble Metals during Oxygen Evolution in Acidic  
345 Media. *ChemCatChem* **6**(8), 2219-2223 (2014).
- 346 31. Dong, C. *et al.* Size-dependent activity and selectivity of carbon dioxide  
347 photocatalytic reduction over platinum nanoparticles. *Nat. Commun.* **9**, 1252  
348 (2018).
- 349 32. Sun, C. & Xue, D. In situ IR spectral observation of  $\text{NH}_4\text{H}_2\text{PO}_4$  crystallization:  
350 structural identification of nucleation and crystal growth. *J. Phys. Chem. C* **117**,  
351 19146-19153 (2013).
- 352 33. Ennis, C., Auchettl, R., Ruzi, M. & Robertson, E. G. Infrared characterisation  
353 of acetonitrile and propionitrile aerosols under Titan's atmospheric conditions.  
354 *Phys. Chem. Chem. Phys.* **19**, 2915-2925 (2017).
- 355 34. Li, Y. H. *et al.* Unidirectional suppression of hydrogen oxidation on oxidized  
356 platinum clusters. *Nat. Commun.* **4**, 2500 (2013).

- 357 35. Chaudhuri., P. *et al.* Electronic structure of bis(o-  
358 iminobenzosemiquinonato)metal complexes (Cu, Ni, Pd). The art of  
359 establishing physical oxidation states in transition-metal complexes containing  
360 radical ligands. *J. Am. Chem. Soc.* **123**, 2213-2223 (2001).
- 361 36. Siemer, N. *et al.* Atomic scale explanation of O<sub>2</sub> activation at the Au-TiO<sub>2</sub>  
362 interface. *J. Am. Chem. Soc.* **140**, 18082-18092 (2018).
- 363 37. Han, G. *et al.* Visible-light-driven valorization of biomass intermediates  
364 integrated with H<sub>2</sub> production catalyzed by ultrathin Ni/CdS uanosheets. *J. Am.*  
365 *Chem. Soc.* **139**, 15584-15587 (2017).
- 366 38. Xiao, J. *et al.* Integration of Plasmonic Effects and Schottky Junctions into  
367 Metal Organic Framework Composites: Steering Charge Flow for Enhanced  
368 Visible-Light Photocatalysis. *Angew. Chem. Int. Ed.* **57**(4), 1103-1107 (2017).
- 369 39. Frens, G Controlled Nucleation for the Regulation of the Particle Size in  
370 Monodisperse Gold Suspensions. *Nat. Phys. Sci.* **241**, 20-22 (1973).
- 371 40. P. C. Lee and D. Miesel. Adsorption and Surface-Enhanced Raman of Dyes on  
372 Silver and Gold Sols. *J. Phys. Chem.* **86**, 3391-3395 (1982).
- 373 41. Liu, L., Gao, F., Zhao, H. & Li, Y. Tailoring Cu valence and oxygen vacancy  
374 in Cu/TiO<sub>2</sub> catalysts for enhanced CO<sub>2</sub> photoreduction efficiency. *Appl. Catal.*  
375 *B-Environ.* **134-135**, 349-358 (2013).

376

377 **Acknowledgments** This work was supported by the National Natural Science  
378 Foundation of China (21876114, 21761142011), Shanghai Government  
379 (19DZ1205102, 19160712900, 18JC1412900), Chinese Education Ministry Key  
380 Laboratory and International Joint Laboratory on Resource Chemistry, and Shanghai  
381 Eastern Scholar Program. Shanghai Engineering Research Center of Green Energy  
382 Chemical Engineering (18DZ2254200). A patent has been filed to protect the method.

383 **Author Contributions** Y.C., M.J.X., Z.F.B. and H.X.L. conceived the idea for the  
384 paper. Y.C., Z.F.B. and H.X.L. designed the experiments. Y.C., J.Y.W., Y.W.  
385 synthesized the material. Q.F.Z., Y.D., X.C. and Z.L.W. performed the HAADF STEM  
386 images. Y.C. performed the sample characterization. Z.F.B., Z.L.W and H.X.L.  
387 conducted the experiments. Y.C., Z.F.B. and H.X.L. analyzed the data and wrote the  
388 manuscript. All authors contributed to writing the paper.

389 **Competing interests** The authors declare no competing interests. Author Information  
390 Reprints and permissions information is available at [www.nature.com/reprints](http://www.nature.com/reprints). Readers  
391 are welcome to comment on the online version of the paper. Correspondence and  
392 requests for materials should be addressed to Z.L.W. ([zlwang@gatech.edu](mailto:zlwang@gatech.edu)), H.X.L.  
393 ([hexing-li@shnu.edu.cn](mailto:hexing-li@shnu.edu.cn)) or Z.F.B. ([bianzhenfeng@shnu.edu.cn](mailto:bianzhenfeng@shnu.edu.cn)).

# Figures

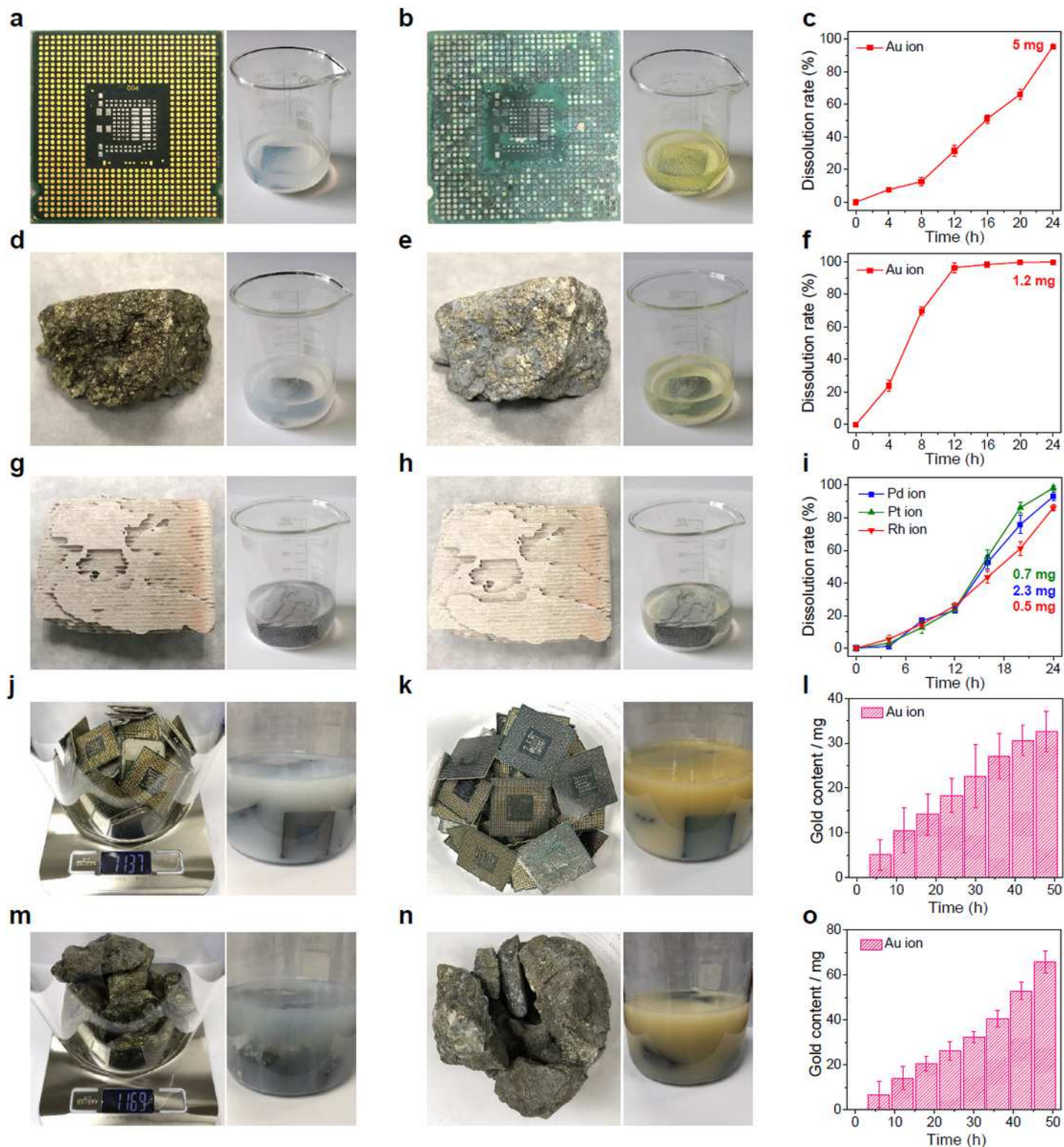


**Figure 1**

Photocatalytic dissolution of precious metals from CPU board, gold ore and TWC. Photographs of retrieving gold from CPU board (a) before and (b) after reaction. Photographs of retrieving gold from gold ore (28.8 g) (d) before and (e) after reaction. Photographs of retrieving precious metals from TWC (17.9



g) (g) before and (h) after reaction. Photographs of retrieving gold from CPU board (1.137 kg) (j) before and (k) after reaction. Photographs of retrieving gold from ore (1.169 kg) (m) before and (n) after reaction. The amount of precious metals obtained by photocatalyzing unbroken CPU board (c) (l), gold ore (f) (o) and TWC (i).

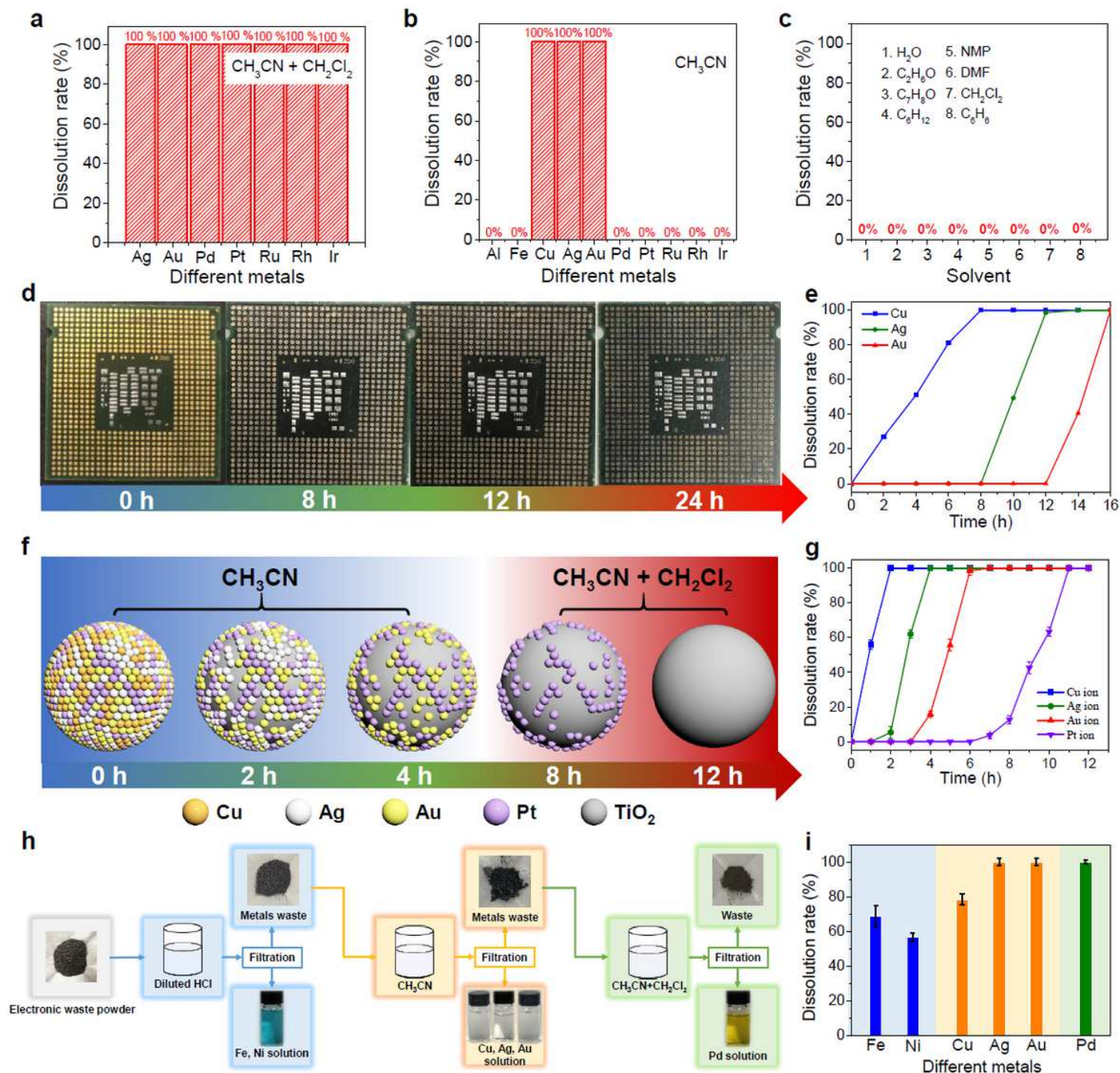


**Figure 2**

Photocatalytic selective dissolution of metals. (a) Dissolution rate of Ag, Au, Pd, Pt, Ru, Rh and Ir in the mixed system of MeCN and DCM under photocatalytic conditions. (b) Dissolution rate of Al, Fe, Cu, Ag, Au, Pd, Pt, Ru, Rh and Ir in MeCN under photocatalytic conditions. (c) Dissolution rate of Au in different

solution. (d) Photographs of selective retrieving metal from CPU board. (f) Schematic diagram of selective dissolution process of metals catalyst (1% Cu/TiO<sub>2</sub>, 1% Ag/TiO<sub>2</sub>, 1% Au/TiO<sub>2</sub> and 1% Pt/TiO<sub>2</sub>). (h) Flow-sheet of stepwise extraction of Fe, Ni, Cu, Ag, Au and Pd from e-waste powder. The amount of metals obtained by selective photocatalyzing (e) CPU board, (g) metals catalyst and (i) e-waste powder.

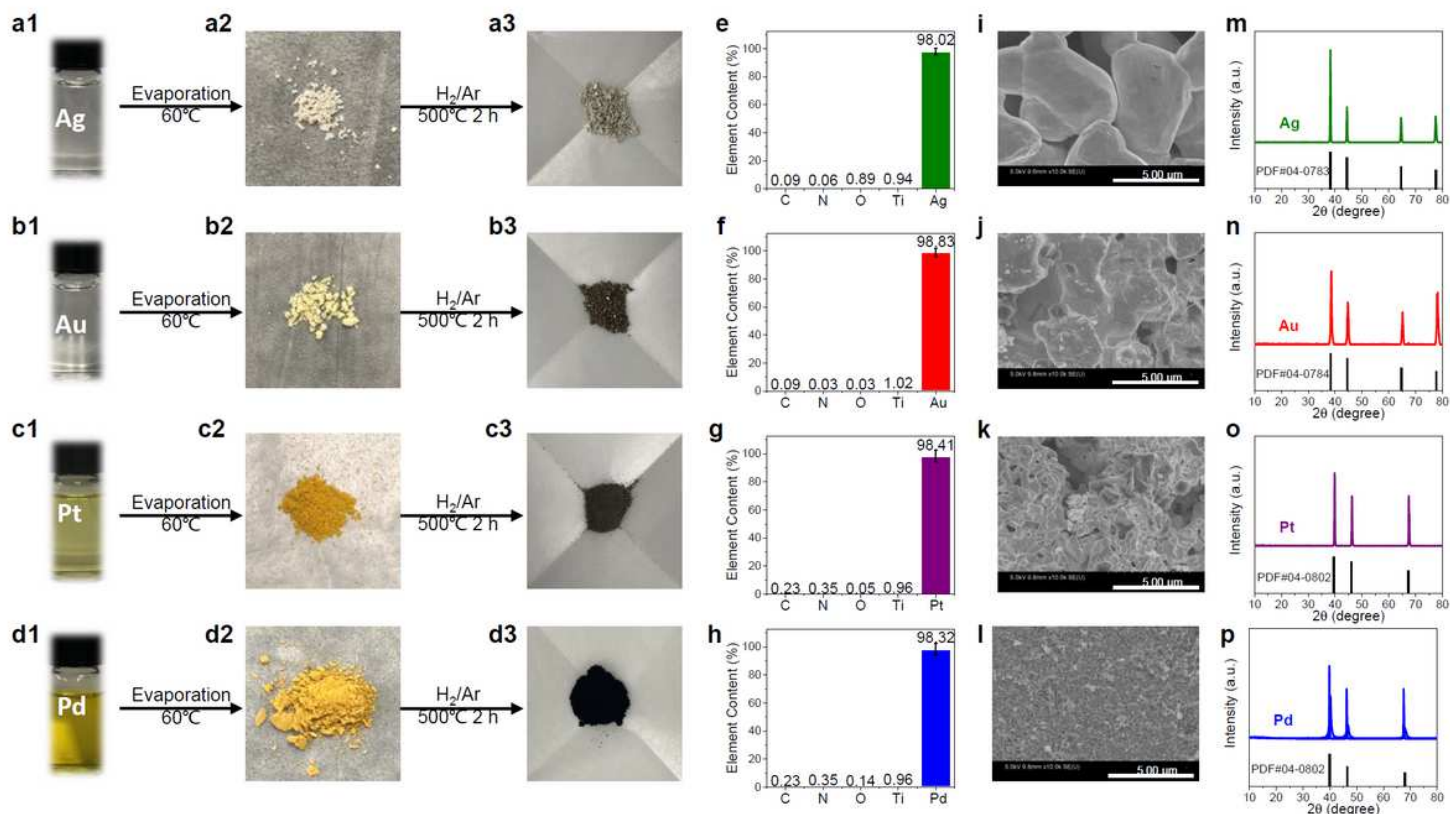


**Figure 3**

Precious metal ion reduction process. The solvent of the dissolved product is removed and then calcined in a reducing atmosphere to obtain metal (a) Ag, (b) Au, (c) Pt and (d) Pd. The proportion of metal elements in the (e) Ag, (f) Au, (g) Pt and (h) Pd after roasting. SEM image of the reduced product (i) Ag, (j) Au, (k) Pt and (l) Pd. XRD pattern of the reduced product (m) Ag, (n) Au, (o) Pt and (p) Pd.



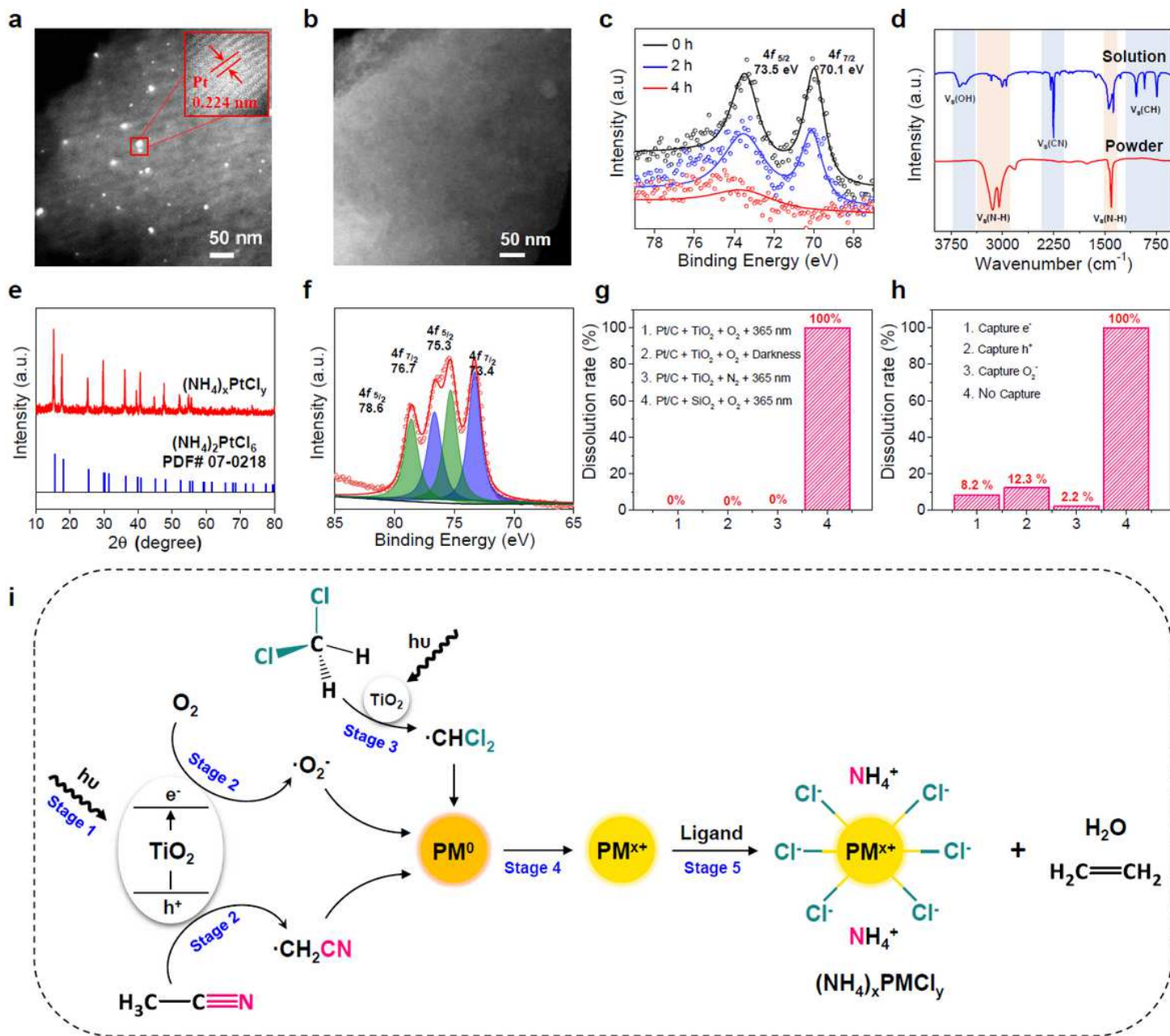


**Figure 4**

Exploration of mechanism. High-angle annular dark-field (HAADF) scanning transmission electron microscopy (STEM) images of 5% Pt/C (a) before and (b) after reaction. (c) The Pt element distribution in Pt/C sample determined by XPS spectra with reaction time. (d) FTIR spectra of solution and powder sample after reaction. (e) XRD patterns and (f) Pt 4f<sub>7/2</sub> XPS spectra of Pt compound obtained from the solution. (g) Dissolution rate of Pt under different conditions. (h) Dissolution rate of Pt under the capture of different living species (DDQ capture electrons (e<sup>-</sup>), EDTA-2Na capture holes (h<sup>+</sup>), p-benzoquinone capture superoxide radical (·O<sub>2</sub><sup>-</sup>)). (i) Proposed mechanism for the retrieving precious metal by photocatalysis.

## Supplementary Files

This is a list of supplementary files associated with this preprint. Click to download.

- [Supplementaryinformation.pdf](#)